Electronic Supplementary Material (ESI) for Chemical Communications.

Supplementary Information

Preparation of ultrasmall cyclodextrin nanogels by an inverse emulsion method using a cationic surfactant†

Satomi Takeuchi,[a] Andrea Cesari,[b] Suzuka Soma,[a] Yota Suzuki,[a] Maria Antonietta Casulli,[a] Kai Sato,[a] Fabrizio Mancin,[b] Takeshi Hashimoto,[a] Takashi Hayashita[a]

[a] *Department of Materials and Life Sciences, Faculty of Science and Technology, Sophia University, 7-1, Kioi-cho, Chiyoda-ku, Tokyo 102-8554, Japan*

[b] *Department of Chemical Sciences, University of Padova, via Marzolo 1, 35131 Padova, Italy*

Materials and Instruments

[Dilauryl(dimethyl)ammonium] bromide (DDAB) was purchased from Tokyo Chemical Industry Co., LTS (Tokyo, Japan) and used without further purification. Native *γ*-cyclodextrin (*γ*-CyD) and acetone was purchased from Kanto Chemical Co., Inc. (Tokyo, Japan). Sodium hydroxide (NaOH), toluene, ethylene glycol diglycidyl ether (EGDE), 1-hexanol were obtained as special-grade reagents from Fujifilm Wako Pure Chemical Corp. (Osaka, Japan). All other organic solvents and reagents were commercially available with guaranteed grade and used as received. Water was doubly distilled and deionized by a Milli-Q water system (WG222, Yamato Scientific Co., Ltd. Tokyo, Japan and Milli-Q Advantage, Merck Millipore, MA, USA) before use.

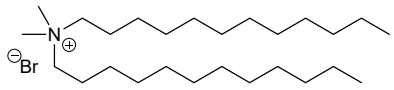

DDAB

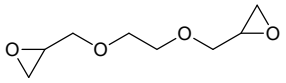

EGDE

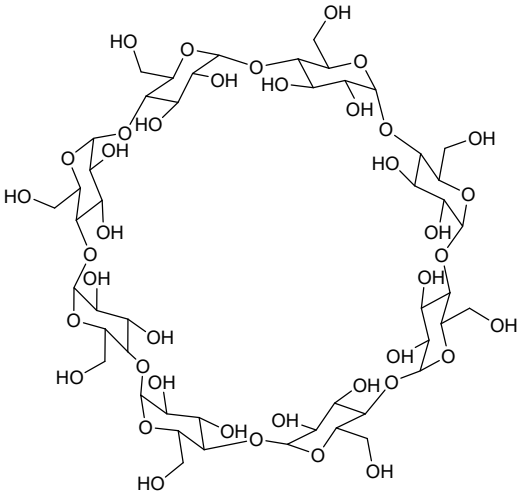

γ-CyD

Chart S1 Structures of DDAB, EGDE, and γ-CyD.

NMR experiments were performed at 25 °C on a Bruker AVANCE III spectrometer operating at 500.13 MHz for ^{1}H and 126 MHz, equipped with a 5 mm z-gradient broad-band inverse (BBI) non-cryogenic probe, and 600 MHz. All deuterated solvents were purchased from Sigma-Aldrich. Dynamic light scattering (DLS) and zeta potential measurements were conducted using Zetasizer Nano ZS (Malvern Instruments Ltd, Malvern, Worcestershire, United Kingdom) at 25 °C. For the DLS measurement, quartz cells (DTS2145 and ZEN2112) were used. For the zeta potential measurement, a disposable cell (DTS1070) was used. Fluorescence spectra were recorded on a HITACHI F-7000 fluorescence spectrophotometer (Hitachi High-Technologies, Co., Tokyo, Japan) at 25 °C with a quartz cell with optical length of 1 cm. Absorbances were recorded using HITACHI U-3900H (Hitachi High-Technologies, Co., Tokyo, Japan) at 25 °C. TEM images were obtained using a transmission electron microscope (JEM-1400 Flash, JEOL) with negative staining. The sample was dropped to a copper-coated formvar grid and then left for 2 minutes. The excess solvent was removed by capillary action using a filter paper. The grids were stained by immersing in 1% uranyl acetate for 2 minutes.

Synthesis of nanogel

Water-in-oil heterogeneous gelation can be used to synthesize nanogels directly from natural polysaccharides by using crosslinking reactions.[1,2] Such method was adopted by Moya-Ortega et al.[3] to obtain hydroxypropyl-β-CyDs and ***γ*-CyDngs** where the crosslinking occurs simultaneously to the emulsification. Moreover, it was proven that CDs can directly react with bifunctional epoxide groups, such as EGDE, to form networks.

In order to emulsify an aqueous CyD solution with a crosslinking agent in an oily phase, two steps are required: (i) emulsifying the CyD solution with an appropriate surfactant; (ii) treating the emulsion with an appropriate pH to produce nanogels by the crosslinking reaction. As the nanogels are incorporated into the internal phase of the emulsion, they adopt the spherical morphology of droplets. Emulsion energy as well as the nature and amount of the surfactant influence the size of the spheres.[1]

The details of the procedure for the formation of ***γ*-CyDngs** are described as follows.

Native *γ*-CyDs (0.33 mmol) were diluted in 5 mL of 0.2 M NaOH. In another beaker, 0.143 mmol of DDAB were diluted in 14.3 mL of toluene. 3 mL of ethylene glycol diglycidyl ether (EGDE) crosslinker were added in the alkaline aqueous solution containing the native *γ*-CyDs. After sonication, 2.5 mL of 1-hexanol were added very slowly. Afterwards, toluene containing DDAB was added to the *γ*-CyDs alkaline aqueous solution. After 15 minutes of standing, homogenization of the solutions was achieved for 10 minutes (homogenizer setting parameters: output control 2.5; duty cycle 50) and the solution was left stirring for 27 hours at room temperature (Scheme S1).

Scheme S1 Preparation of ***γ*-CyDngs.**

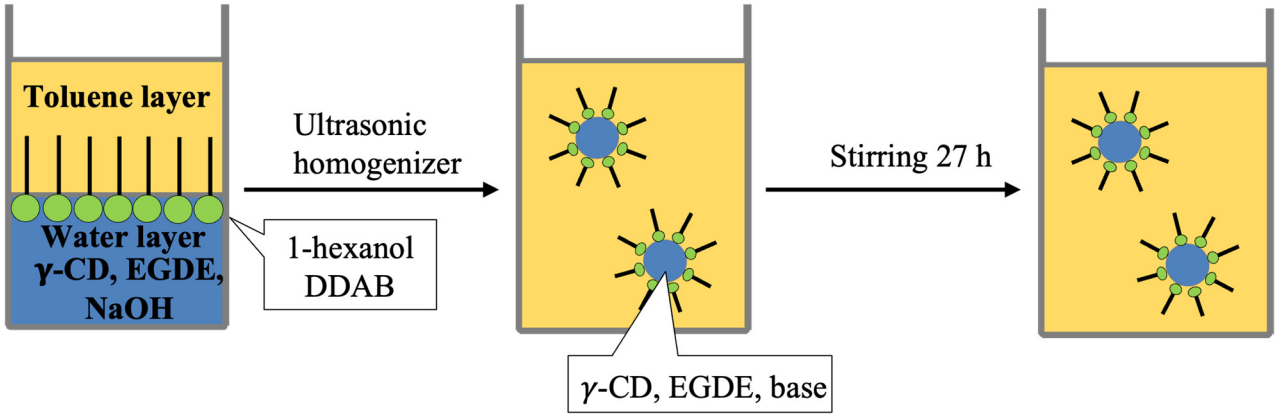

After having picked up the water part containing the nanogels, 20 mL of acetone were added. By performing a centrifugation, (at 10 000 rpm for 10 minutes) the toluene and the surfactant residuals moved to the acetone part. After that, the pH was adjusted from basic to neutral one, through the addition of hydrochloric acid (HCl). Dialysis was carried out first in ion water and then in Milli-Q water for 7 days. Two kinds of filtration were achieved in series: the first one by using a paper filter of 1 µm pores, subsequently with a membrane filter of 450 nm pores. (In some preliminary experiments, the membrane filtration was not conducted.) After having freeze dried, ***γ*-CyDngs** were obtained and diluted in Milli-Q water to 15 mg/mL.

Optimization of the reaction time

For the polymerisation reaction, the homogenised suspension was stirred at room temperature, and this was followed by purification of the formed nanogels by dialysis and membrane filtration. It should be noted that the morphology of the nanogels is sensitive to the reaction time (Table S1). A polymerisation time shorter than 12 hours is not sufficient for nanogel formation, whereas polymerisation over 48 hours leads to the formation of macrogels that are difficult to disperse in water (Fig. S1). Therefore, the optimal polymerisation time was set to 27 hours for the preparation of ultrasmall nanogels (≈10 nm) with a sufficiently hydrophobic space, due to the CyD cavities and to the interstitial space between the CyDs, to enable the inclusion of hydrophobic compounds, such as fluorescent molecules, probes, and drugs.

Table S1 DLS data of ***γ*-CyDngs** prepared with various reaction times. [a]

Stirring time / hours	Diameter [b] / nm	Zeta potential [c] / mV	Yield / g
3	2.07±1.29	−2.21±0.81	0.142
6	3.17±0.42	−6.21±2.42	0.252
9	3.11±2.34	−4.09±0.70	0.243
12	4.60±1.90	−0.03±1.17	0.534
15	6.33±0.44	−2.61±0.34	0.606
18	7.22±1.25	−2.59±0.21	0.527
21	5.76±1.14	−3.20±0.05	0.506
24	5.28±1.26	−0.63±0.55	0.616
27	6.54±0.76	−1.61±0.20	0.349
30	11.55±3.13	−3.00±0.29	0.465

a. This measurement was conducted as a preliminary experiment; the ***γ*-CyDngs** used here were not filtered with a membrane.

b. Determined from number-size distributions.

c. Measured in non-buffered water.

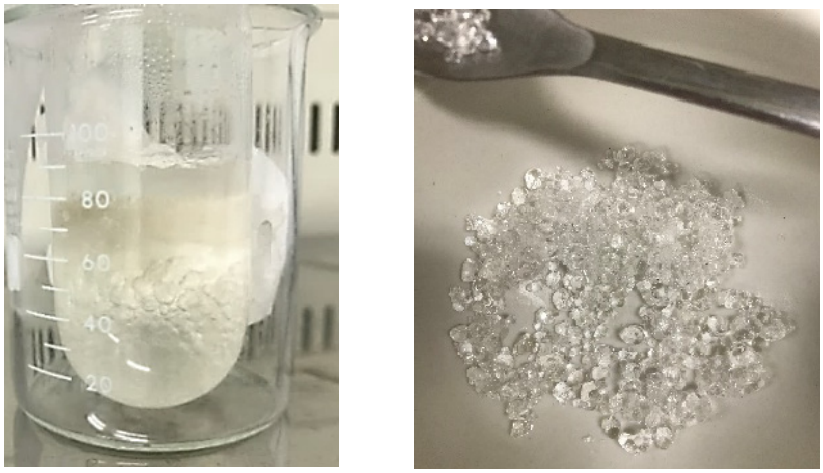

Fig. S1 Photographs of ***γ*-CyDngs** obtained after 48 hours of polymerisation.

TEM images

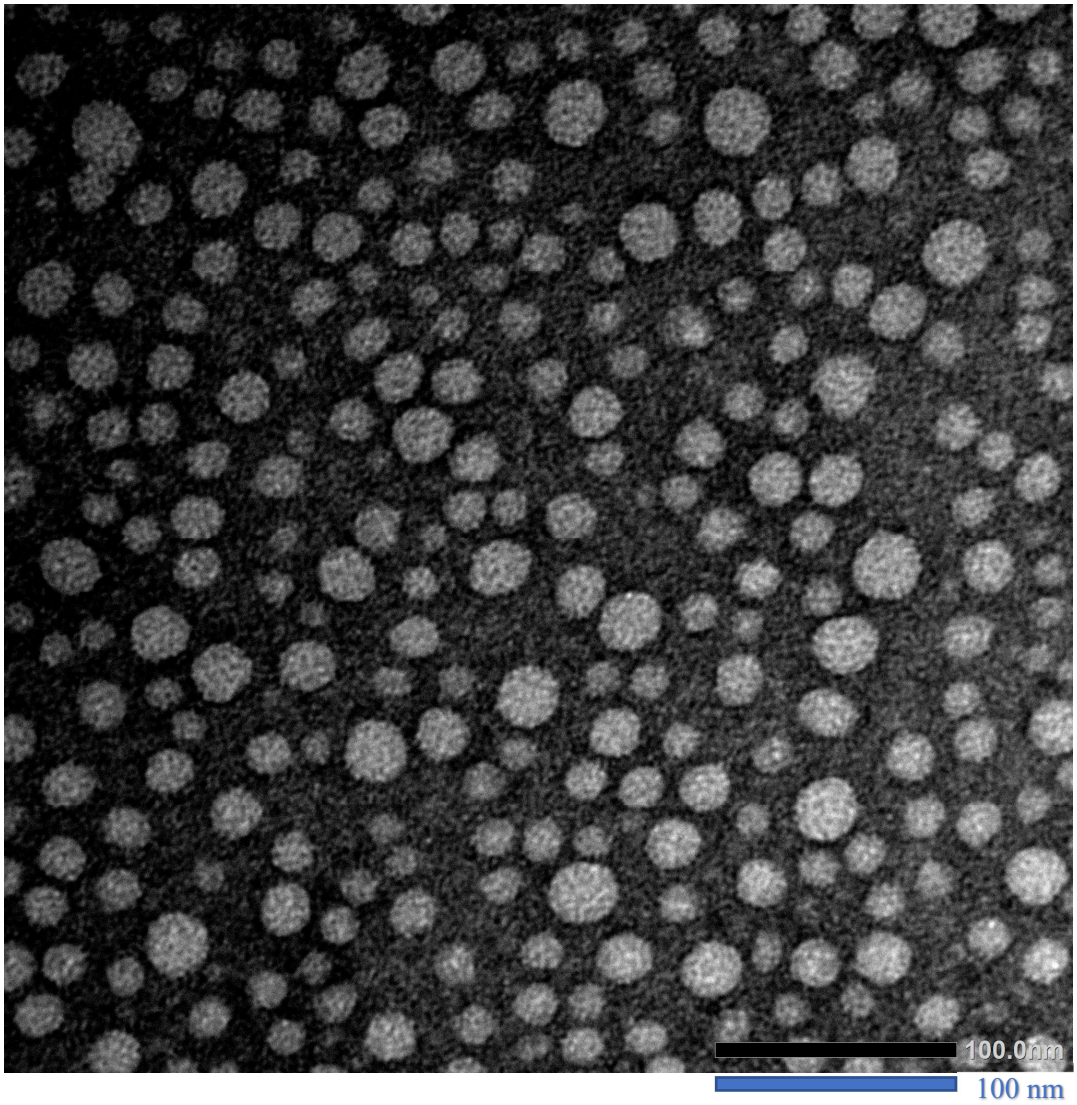

Fig. S2. Enlarged TEM image of ***γ*-CyDngs** (Fig. 1 in the manuscript).

DLS measurement

(a)

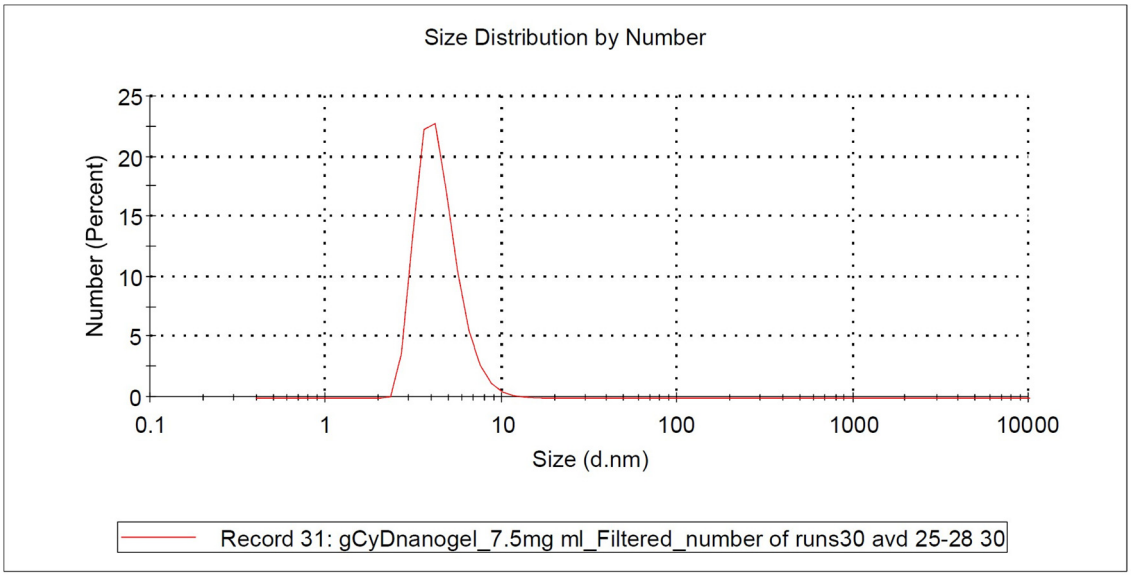

(b)

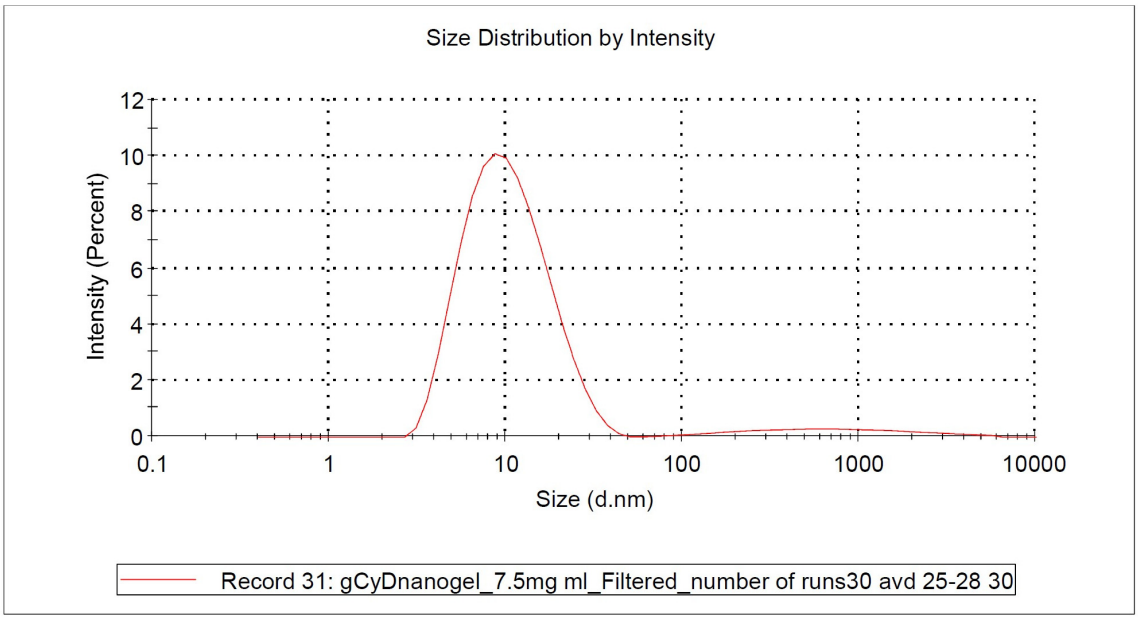

Fig. S3. Number- (a) and intensity- (b) size distributions of ***γ*-CyDngs** (7.5 mg/mL) at 25 °C in water. The distributions represent the averages of five individual measurement data. The intensity diameter was determined to be 11.39 ± 6.3 nm in (b).

Turbidity

Table S2 Turbidity of the ***γ*-CyDngs**.

Concentration of ***γ*-CyDngs** / mg mL^{-1}	Absorbance at 600 nm
5	0.0010
10	0.0016
15	0.0019
20	0.0037
40	0.0029
60	0.0076
80	0.0086
100	0.0097

Table S3 DLS data of ***γ*-CyDngs** prepared in the presence and absence of DDAB.[a]

Entry	Diameter (nm) [a]	PdI	Zeta potential / mV [c]
Preparation with DDAB	6.54±0.76	0.65±0.01	-1.61±0.20
Preparation without DDAB	5.34±2.33	1.00	-3.96±0.36

a. This measurement was conducted as a preliminary experiment; the ***γ*-CyDngs** used here were not filtered with a membrane.

b. Determined from number-size distributions.

c. Measured in non-buffered water.

Zeta-potential

Table S4 Zeta potential of ***γ*-CyDngs** in water under various pH condition with the corresponding DLS data.

pH	Diameter / nm [a]	Zeta potential / mV [b]
3	12.84±2.66	−0.36±0.54
4	7.33±1.20	−0.63±0.96
5	5.24±1.71	−0.70±0.71
6	7.55±2.26	−1.15±0.80
7	6.38±2.73	−1.85±0.41
7.4	7.03±1.64	−0.91±0.45
8	7.88±3.05	−1.55±0.54
9	10.84±2.54	−2.18±1.10
10	6.95±2.05	−1.62±0.17
11	7.11±2.86	−1.35±0.44
12	8.40±4.62	−4.12±0.79

a. Determined from number-size distributions.

b. Measured in the presense of HEPES buffer (5 mM).

Table S5 Zeta potential of **EGDEngs** in water under various pH condition with the corresponding DLS data.

pH	Diameter / nm [a]	Zeta potential / mV [b]
3	3.53±1.16	−0.80±1.29
4	3.70±1.48	−2.13±0.62
5	4.07±1.00	−2.21±0.36
6	3.61±1.14	−2.66±1.58
7	4.82±0.46	−2.90±0.73
7.4	4.59±0.65	−2.73±1.15
8	4.46±0.76	−3.36±1.58
9	4.31±0.45	−1.21±1.29
10	3.85±1.26	−3.82±0.98
11	3.74±1.31	−1.89±1.04
12	3.22±1.53	−2.79±0.77

a. Determined from number-size distributions.

b. Measured in the presense of HEPES buffer (5 mM).

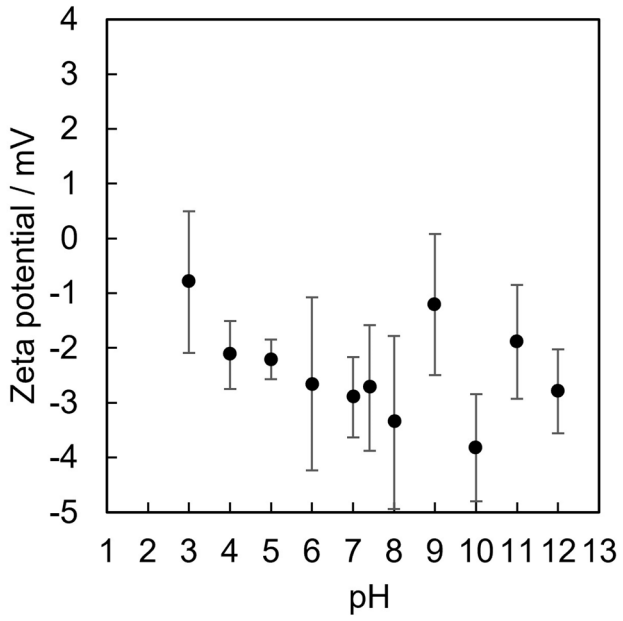

Fig. S4 Zeta potential of **EGDEngs** in water under various pH conditions (n = 5). in water (5 mM HEPES buffer) at 25 °C.

Inclusion constant for γ-CyD with TNS

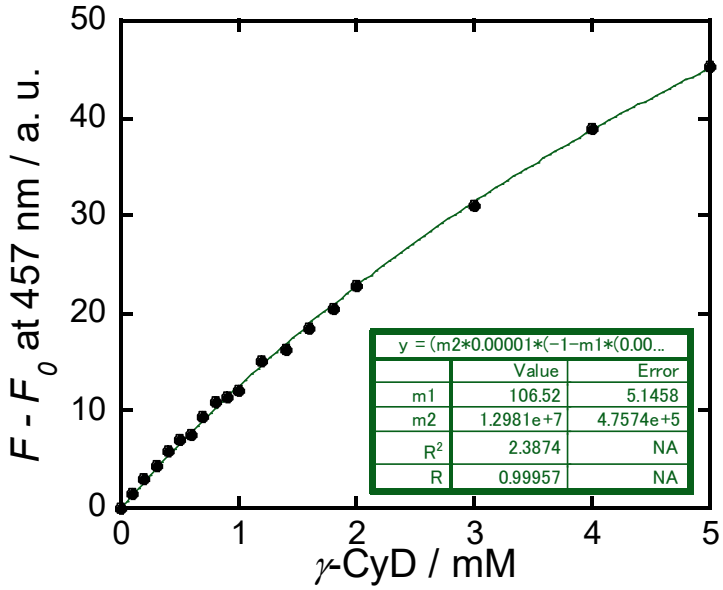

Fig. S5 Change in the fluorescence intensity ($F - F_0$) at 457 nm of TNS with increasing the concentration of γ-CyD in DMSO/water (1/99 in v/v): C_{TNS} = 10 μM, C_{HEPES} = 5 mM, pH 7.4, T = 25 °C, and λ_{ex} = 320 nm. The abbreviations F and F_0 denote the fluorescence intensity of TNS in the presence and absence of γ-CyD, respectively. The experimental plots were fitted by the theoretical equation derived from 1:1 binding model.

The binding model used was derived as follows. The equilibrium between TNS (G) and γ-CyD (CyD) can be expressed as Equation S1.

$$\mathrm{G} + \mathrm{CyD} \underset{}{\overset{K_{11}}{\rightleftharpoons}} \mathrm{G\text{-}CyD} \qquad \text{(S1)}$$

Therefore,

$$K_{11} = \frac{[\mathrm{G\text{-}CyD}]}{[\mathrm{G}][\mathrm{CyD}]} \qquad \text{(S2)}$$

$$[\mathrm{G}]_t = [\mathrm{G}] + [\mathrm{G\text{-}CyD}] \qquad \text{(S3)}$$

$$[\mathrm{CyD}]_t = [\mathrm{CyD}] + [\mathrm{G\text{-}CyD}] \qquad \text{(S4)}$$

in which, $[\mathrm{G}]_t$ and $[\mathrm{CyD}]_t$ denote the total concentrations of TNS and γ-CyD, respectively.

Fluorescence intensity at a specific wavelength (F) can be expressed as Equation S5.

$$F = \beta_{G}[G] + \beta_{G\text{-}CyD}[G\text{-}CyD] \tag{S5}$$

in which, β_G and $\beta_{G\text{-}CyD}$ denote propotional coefficients for [G] and [G-CyD], respectively, corresponding to the emission intensities per 1 mol.

According to Equations S2 and S3,

$$[G]_t = \frac{[G\text{-}CyD]}{K_{11}[CyD]} + [G\text{-}CyD] = \frac{[G\text{-}CyD]}{K_{11}[CyD]} \cdot (1 + K_{11}[CyD]) \tag{S6}$$

$$\therefore [G\text{-}CyD] = \frac{K_{11}[CyD][G]_t}{1 + K_{11}[CyD]} \tag{S7}$$

By substituting Equation S7 into Equation S4, Equation S8 is given.

$$[CyD]_t = [CyD] + \frac{K_{11}[CyD][G]_t}{1 + K_{11}[CyD]} \tag{S8}$$

$$\therefore [CyD]_t = \frac{[CyD] + K_{11}[CyD]^2}{1 + K_{11}[CyD]} + \frac{K_{11}[CyD][G]_t}{1 + K_{11}[CyD]} \tag{S9}$$

$$\therefore (1 + K_{11}[CyD])[CyD]_t = K_{11}[CyD]^2 + K_{11}[G]_t[CyD] + [CyD] \tag{S10}$$

$$\therefore K_{11}[CyD]^2 + \{1 + K_{11}([G]_t - [CyD]_t)\}[CyD] - [CyD]_t = 0 \tag{S11}$$

$$\therefore [CyD] = \frac{-\{1 + K_{11}([G]_t - [CyD]_t)\} + \sqrt{\{1 + K_{11}([G]_t - [CyD]_t)\}^2 + 4K_{11}[CyD]_t}}{2K_{11}} \tag{S12}$$

According to Equations S2 and S3,

$$[G]_t = [G] + K_{11}[G][CyD] = [G](1 + K_{11}[CyD]) \tag{S13}$$

$$\therefore [G] = \frac{[G]_t}{1 + K_{11}[CyD]} \tag{S14}$$

From Equations S5, S7, and S14,

$$F = \beta_{G} \cdot \frac{[G]_t}{1 + K_{11}[CyD]} + \beta_{G\text{-}CyD} \cdot \frac{K_{11}[CyD][G]_t}{1 + K_{11}[CyD]} \tag{S15}$$

$$\therefore F = \frac{[G]_t \cdot (\beta_G + \beta_{G\text{-}CyD} K_{11}[CyD])}{1 + K_{11}[CyD]} \quad \text{(S16)}$$

As $F_0 = \beta_G[G]_t$, Equation S16 can be rearranged as Equation S17.

$$F - F_0 = \frac{[G]_t \cdot (\beta_G + \beta_{G\text{-}CyD} K_{11}[CyD])}{1 + K_{11}[CyD]} - \beta_G[G]_t \quad \text{(S17)}$$

$$\therefore F - F_0 = \frac{K_{11}[G]_t[CyD] \cdot (\beta_{G\text{-}CyD} - \beta_G)}{1 + K_{11}[CyD]} \quad \text{(S18)}$$

in which F_0 denotes the fluorescence intensity of TNS in the absence of *γ*-CyD. By substituting Equation S12 into Equation S18, Equation S19 is obtained.

$$F - F_0 = \frac{K_{11}[G]_t \cdot \dfrac{-\left\{1 + K_{11}([G]_t - [CyD]_t)\right\} + \sqrt{\left\{1 + K_{11}([G]_t - [CyD]_t)\right\}^2 + 4K_{11}[CyD]_t}}{2K_{11}} \cdot (\beta_{G\text{-}CyD} - \beta_G)}{1 + K_{11} \cdot \dfrac{-\left\{1 + K_{11}([G]_t - [CyD]_t)\right\} + \sqrt{\left\{1 + K_{11}([G]_t - [CyD]_t)\right\}^2 + 4K_{11}[CyD]_t}}{2K_{11}}} \quad \text{(S19)}$$

$$\therefore F - F_0 = \frac{[G]_t \cdot \left\{-1 - K_{11}([G]_t - [CyD]_t) + \sqrt{\left\{1 + K_{11}([G]_t - [CyD]_t)\right\}^2 + 4K_{11}[CyD]_t}\right\} \cdot (\beta_{G\text{-}CyD} - \beta_G)}{1 - K_{11}([G]_t - [CyD]_t) + \sqrt{\left\{1 + K_{11}([G]_t - [CyD]_t)\right\}^2 + 4K_{11}[CyD]_t}} \quad \text{(S20)}$$

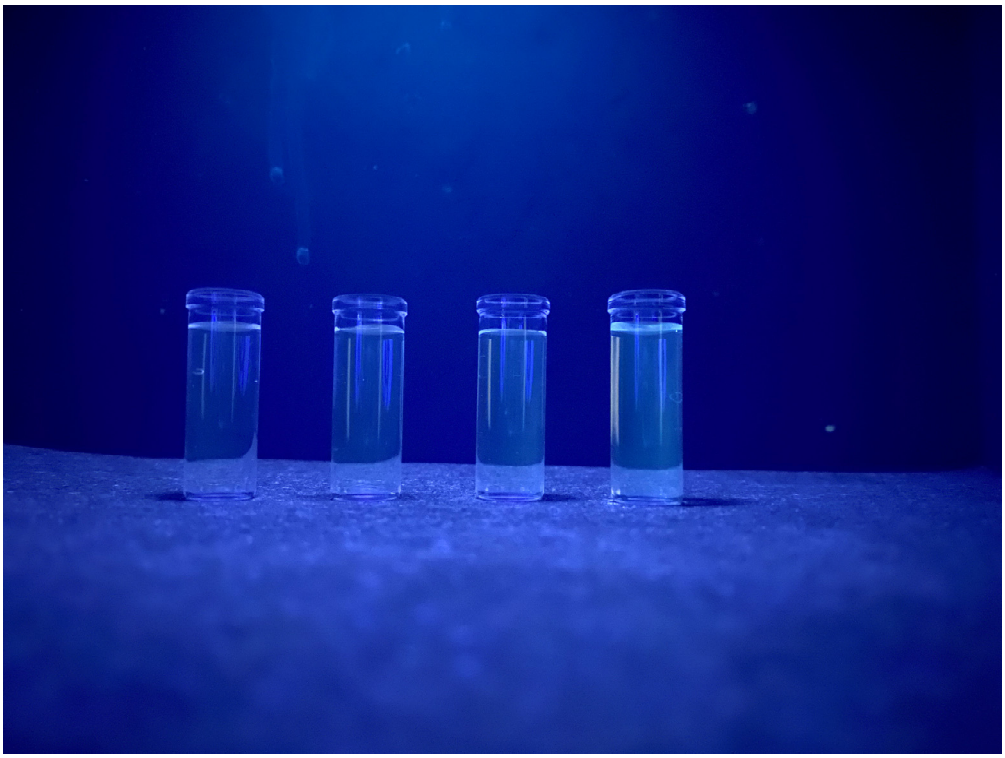

Fig. S6. Images of TNS solutions containing various concentrations of native *γ*-CyD (from left to right: 0, 0.03, 0.3, and 0.9 mg/mL) under 365 nm UV lamp irradiation.

For the TNS fluorescent analysis (Fig. 3 in the manuscript), we can compare the fluorescence intensity in 3.0 mg/mL of native γ-CyD (= 2.3 x 10^{-3} mol/L) solution with that in the same concentration (3.0 mg/mL) of **γ-CyDngs** solution. As shown in the NMR discussion in our manuscript, 74% w/w of γ-CyD was included in the **γ-CyDngs**. Therefore, the apparent concentration of γ-CyD in **γ-CyDngs** solution is calculated to be 1.7 x 10^{-3} mol/L, which is clearly lower than that of native γ-CyD solution (2.3 x 10^{-3} mol/L). However, our **γ-CyDngs** exhibited much stronger fluorescent emission, indicating the superior inclusion affinity of **CyDngs** for TNS.

Langmuir analysis

In Langmuir isotherm model, the adsorption equilibrium between TNS (G) and ***γ*-CyDngs** (H) can be expressed as Equation S21.

$$G + H \underset{}{\overset{K}{\rightleftharpoons}} GH \qquad (S21)$$

in which *K* is the association constant for the equilibrium. From Fig. 2b, the double reciprocal plot between the fluorescence intensity (*F*) and ***γ*-CyDngs** concentration ([H] / mg·ml^{-1}) was drawn (Fig. S7).

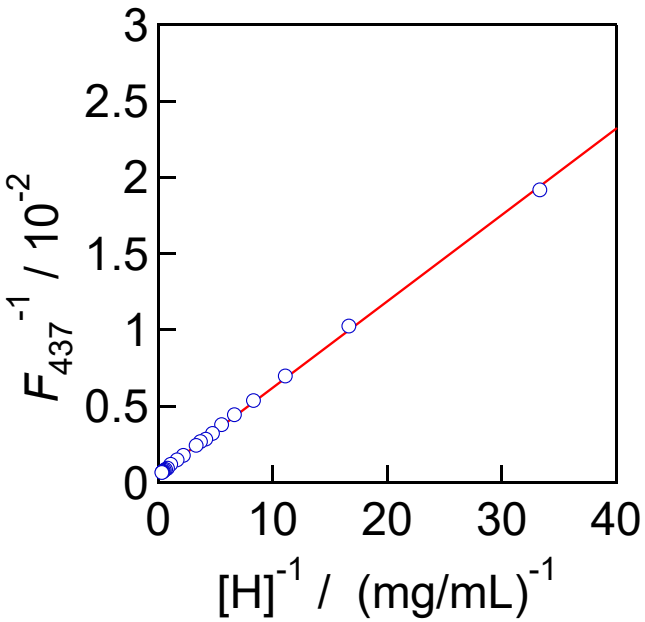

Fig. S7. Double reciprocal plots between the fluorescence intensity and ***γ*-CyDngs** concentration. The data were taken from Fig. 3c in the manuscript.

As it can be seen in Fig. S7, linear relationship is verified between F^{-1} and $[H]^{-1}$. Therefore, Equation S22 is obtained.

$$\frac{1}{F} = a \cdot \frac{1}{[H]} + b \qquad (S22)$$

where, a = 0.000566 and b = 0.000537.

When the saturated *F* in Fig. 3c is defined as F_{max}, Equation S22 is arranged to Equation S23.

$$\frac{1}{F_{max}} = b \qquad (S23)$$

$$\therefore F_{max} = \frac{1}{b} \qquad (S24)$$

F at 437 nm (F_{437}) can be expressed as Equation S25.

$$F_{437} = i_{G}[G] + i_{GH}[GH] \quad \text{(S25)}$$

in which, i_G and i_{GH} are proportional constants. At 437 nm, the fluorescence from G is negligible. Therefore, Equation S25 can be approximated to be Equation S26.

$$F_{437} = i_{GH}[GH] \quad \text{(S26)}$$

When the total concentration of G is defined as C_G, Equation S27 holds.

$$C_{G} = [G] + [GH] \quad \text{(S27)}$$

When the change in the fluorescence intensity is saturated, all G molecules are adsorbed by H. Therefore, Equation S28 is provided.

$$C_{G} \approx [GH] \quad \text{(S28)}$$

According to Equations S26 and S28, Equation S29 is given.

$$F_{max,437} = i_{GH} C_{G} \quad \text{(S29)}$$

$$\therefore i_{GH} = \frac{F_{max,437}}{C_{G}} = \frac{1}{b} \cdot \frac{1}{C_{G}} \quad \text{(S30)}$$

According to Equations S26 and S27, [G] and [GH] can be expressed as follows.

$$\begin{cases} [GH] = bC_{G}F_{437} \\ [G] = C_{G} - bC_{G}F_{437} \end{cases} \quad \text{(S31)}$$

According to Equation S31, the ratio of the number of occupied adsorption sites (r) to the number of sites (n) per 1 g of ***γ*-CyDngs**, i.e., surface coverage, can be expressed as Equation S32.[4]

$$\frac{r}{n} = \frac{[GH]}{[H] + [GH]} = \frac{K[G][H]}{[H] + K[G][H]} = \frac{K[G]}{1 + K[G]} \quad \text{(S32)}$$

Equation S32 can be arranged to Equation S33.

$$\frac{1}{r}=\frac{1+K[G]}{nK[G]}=\frac{1}{nK[G]}+\frac{1}{n} \quad \text{(S33)}$$

From the concentration of nanogel (mg/mL), the [GH] (mol/L) can be converted to *r* (mol/g). By drawing a double reciprocal plot between r and [G] (Fig. S8), *K* and n are determined to be 3.61×10^3 M^{-1} and 1.90×10^{-4} mol/g, respectively.

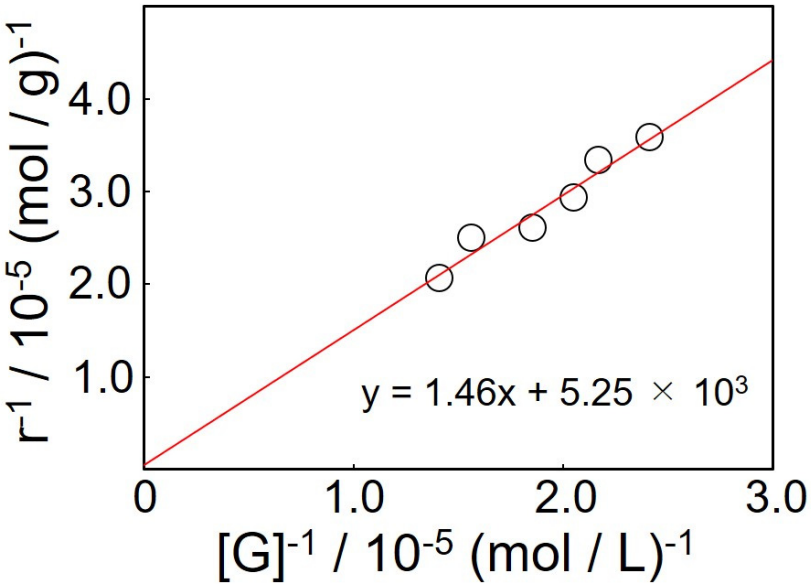

Fig. S8. Double reciprocal plots between r and [G].

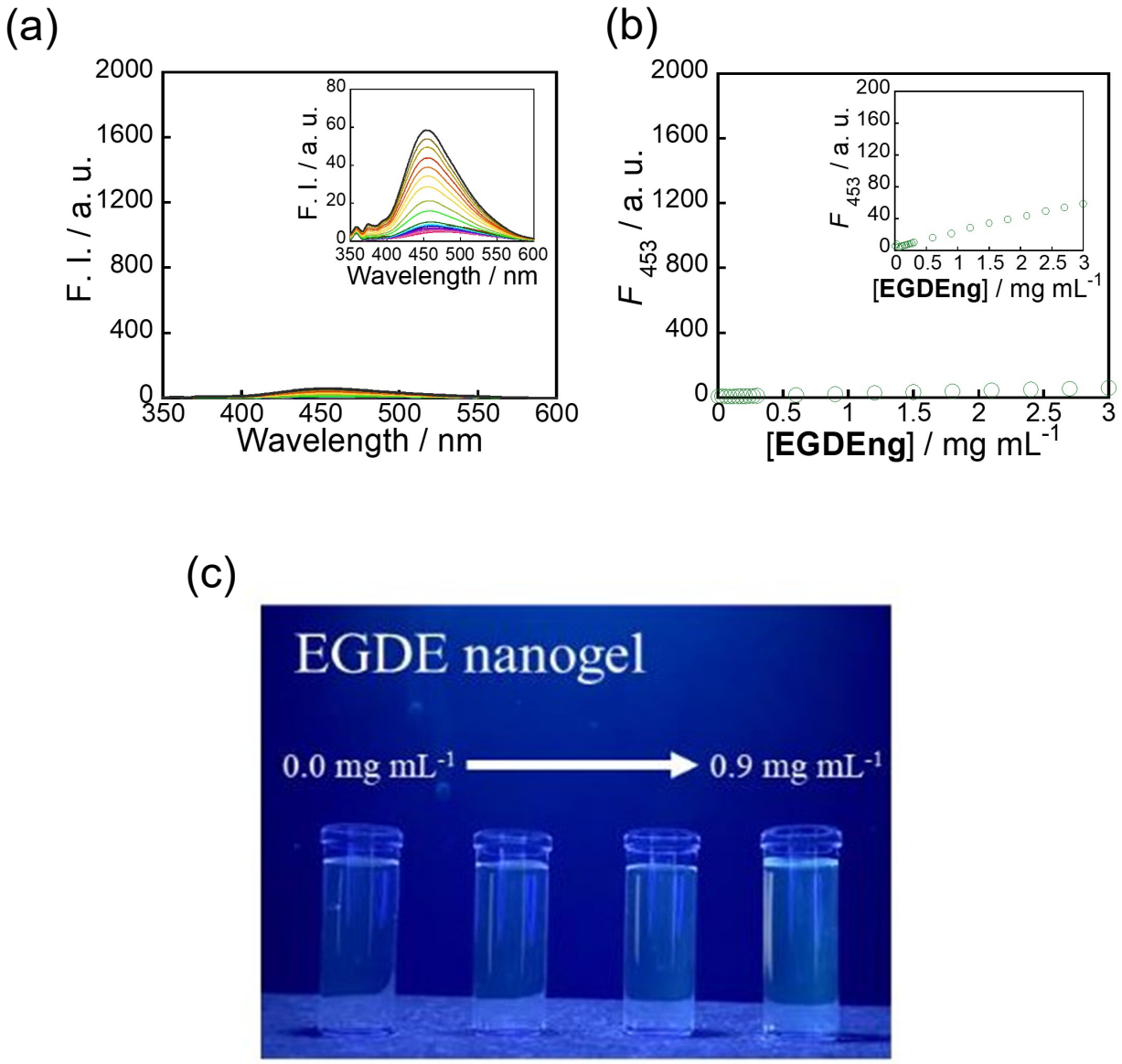

Figure S9 Fluorescence spectra (a) and the intensity at 453 nm (b) of TNS in the presences of various concentrations of **EGDEng**s in DMSO/water (1/99 in v/v): C_{TNS} = 10 μM, pH 7.4, 5 mM HEPES buffer, 25 °C, and λ_{ex} = 320 nm. Photographs of TNS solutions containing various concentrations of **EGDEng** (from left to right: 0, 0.03, 0.3, and 0.9 mg/mL) under 365 nm UV lamp irradiation (c)

Estimation of hydrophobicity

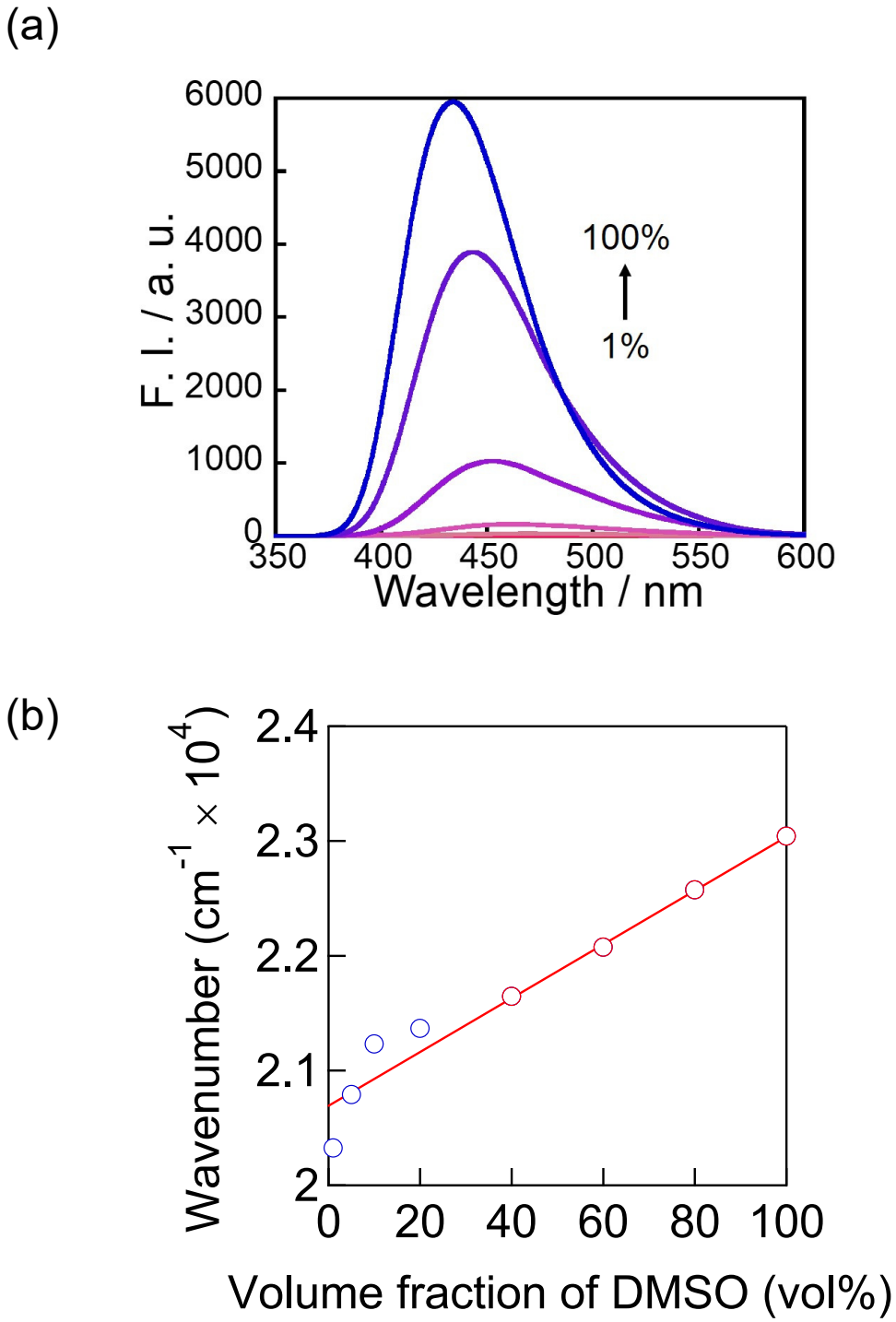

Figure S10 (a) Fluorescence spectra of TNS in a mixture of DMSO and water with various volume fractions. (b) Relationship between wavenumber at fluorescence maximum of TNS and volume fraction of DMSO. The calibration curve was drawn in the range of the DMSO volume fraction from 40 to 100%.

A linear relationship held between wavenumber of fluorescence maximum and volume fraction of DMSO in the range of 40 - 100%. The calibration curve is expressed as Equation S34.

$$y = 23.4\,x + 20700 \qquad \text{(S34)}$$

The plots measured at < 30% DMSO fractions were deviated from the line, plausibly because of complicated behaviour of the solvent polarity for a binary solvent mixture with DMSO and water.[5]

The maximum fluorescence wavelength of TNS with ***γ*-CyDngs** is 437 nm, i.e., 22900 cm^{-1}. Therefore, the hydrophobicity within ***γ*-CyDngs** corresponds to a mixed solvent containing 93% DMSO.

NMR experiments

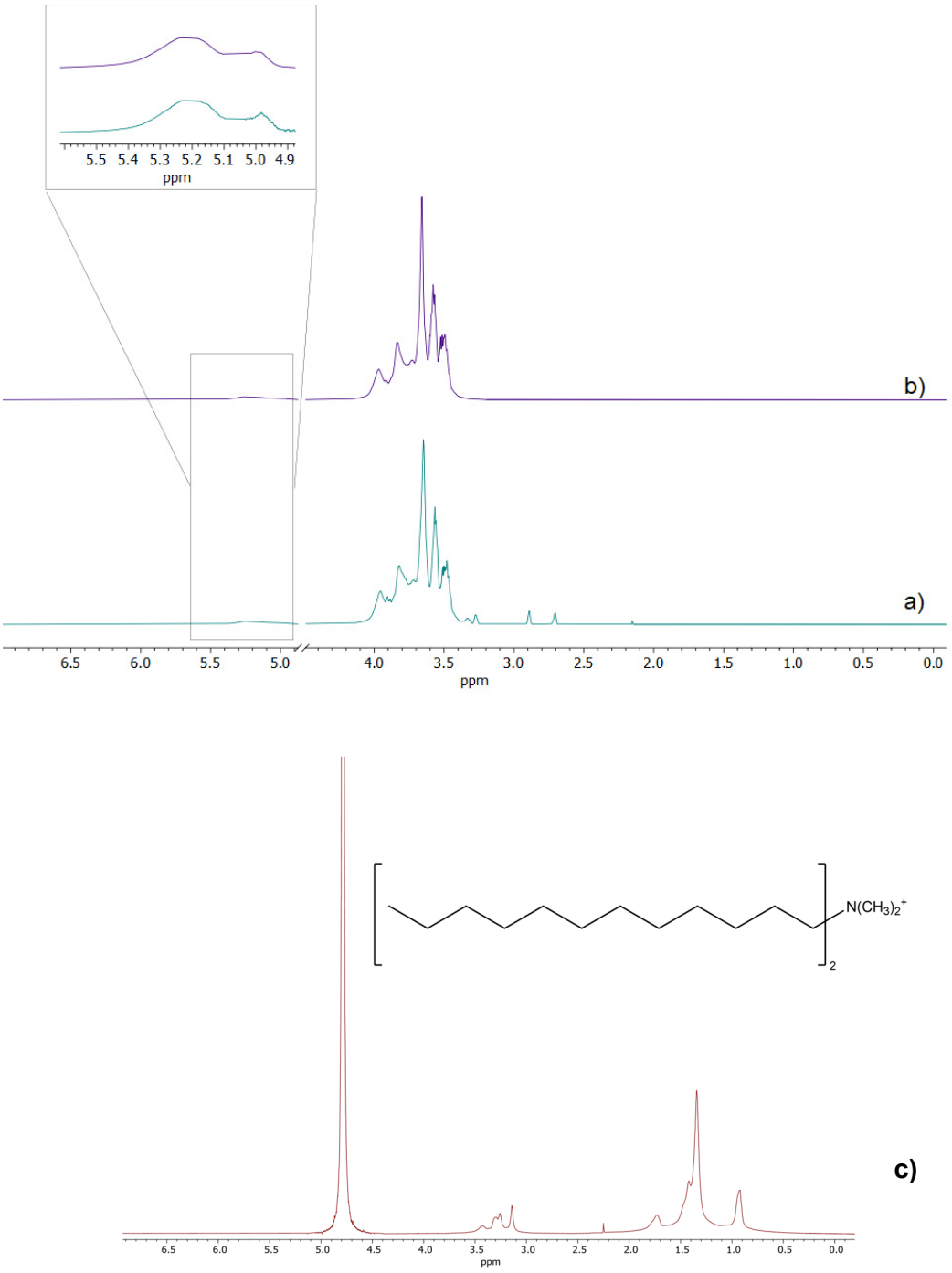

Fig. S11. a) ^{1}H NMR spectrum (500 MHz, 25 °C, D_2O, 10 mM) and b) diffusion filter of ***γ*-CyDngs** together with the ^{1}H NMR spectrum of DDAB in D_2O c). By the comparison of the spectra of a) and c), it is certainly shown that no DDAB remains in ***γ*-CyDngs**.

Hydrodynamic radius from DOSY (Stokes-Einstein equation)

The translational molecular motion in solution is characterized by the parameter *D*, which represents a parameter that can be usefully exploited to detect the interaction between a small molecule and a macromolecule. The dependence of this parameter from the hydrodynamic radius (r_H) and viscosity (η) can be expressed by means of the Stokes–Einstein equation, strictly holds for spherical molecules:

$$D = \frac{k_b T}{6\pi\eta r_H} \qquad \text{(S35)}$$

where k_b is the Boltzmann constant (1.380649 10^{-23} Pa·m^3/K), T (298.15 K) is the absolute temperature, η is the viscosity of the solvent (0.89 10^{-3} Pa·s).

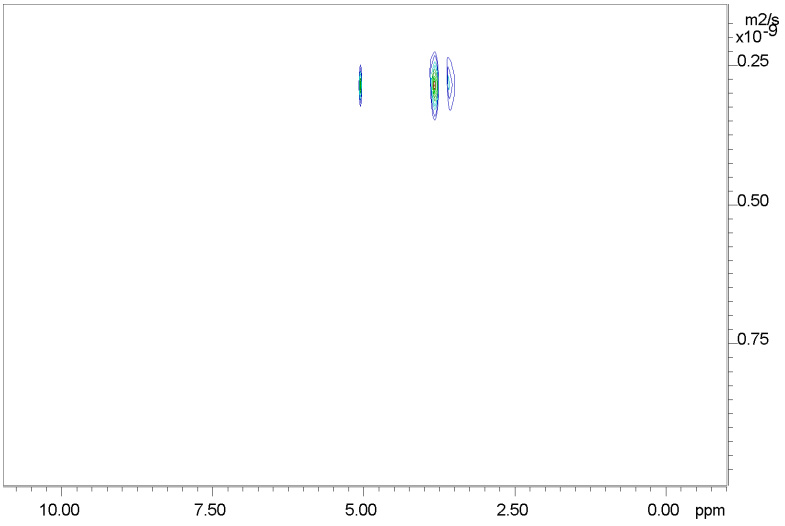

Fig. S12 Pseudo-2D DOSY map (500 MHz, D_2O, 10 mM) of *γ*-CyD**.**

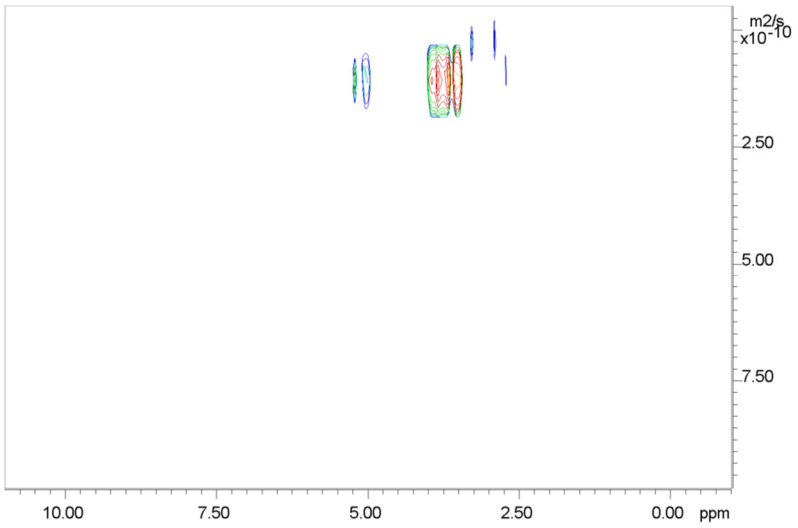

Fig. S13 Pseudo-2D DOSY map (500 MHz, D_2O, 10 mM) of ***γ*-CyDngs.**

Table S6 NMR transverse relaxation times (T_2, s) (500 MHz, 25 °C, D_2O, 10 mM) of *γ*-CyD and ***γ*-CyDngs**.

γ-CyD				***γ*-CyDng**			
	ppm	T_2	err		ppm	T_2	err
H_1	5.14	0.1626	0.0019	H_1	5.233	0.0625	0.0008
H_2	3.68	0.2544	0.0106	H_2-H_6	3.812	0.0955	0.0017
H_3	3.95	0.2602	0.0088	EGDE1	2.99	0.1044	0.0211
H_4	3.62	0.2340	0.0037	EGDE2	2.80	0.1371	0.0307
H_5/H_6	3.88/3.90	0.1665	0.0007				
Average	-	0.216	0.005				

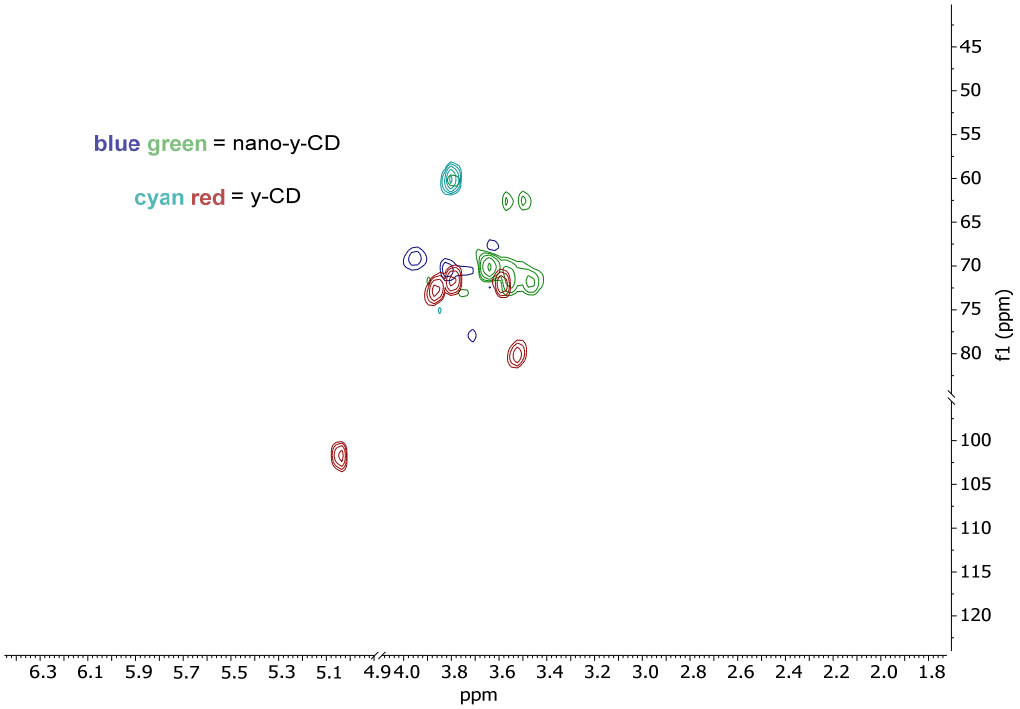

Fig. S14 Superimposition of 2D HSQC maps (600 MHz, D_2O, 10 mM) of *γ*-CyDs (cyan-red) and ***γ*-CyDngs** (blue-green).

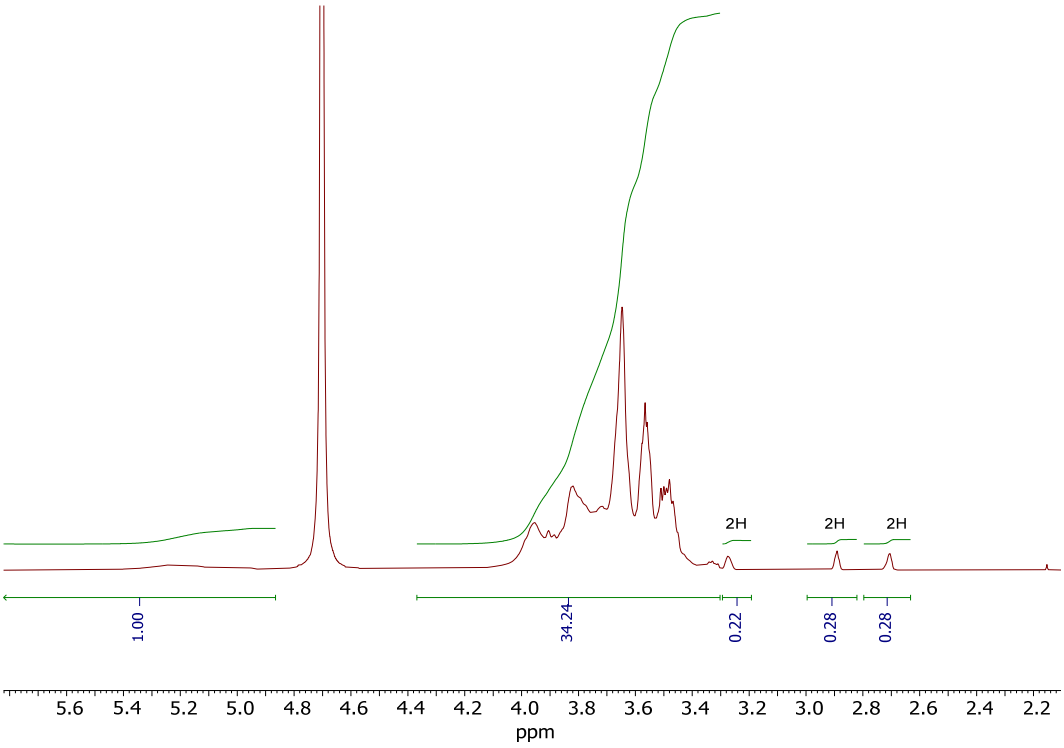

Figure S15 ^{1}H NMR spectrum of (600 MHz, D_2O, 10 mM) ***γ*-CyDngs.**

For the quantification of *γ*-CyDs in ***γ*-CyDngs**, unit was assigned to the integral of the anomeric proton which

therefore counts for a single *γ*-CD molecule. Then, the small contribution of EGDE proton unit belonging to the component defined as “external”, i.e. that has signals similar to epoxide, was calculated dividing by 2 one of the low ppm signals (protons H_5 of EGDE which are well isolated and integrable). Is possible to remove the contributions of the “external” EGDE protons (x11) and of the *γ*-CyD ring protons (x6) within the 3.4÷4.4 ppm region. In this way, is possible to calculate the remained contribution of “inner” EGDE, and hence its proton unit.

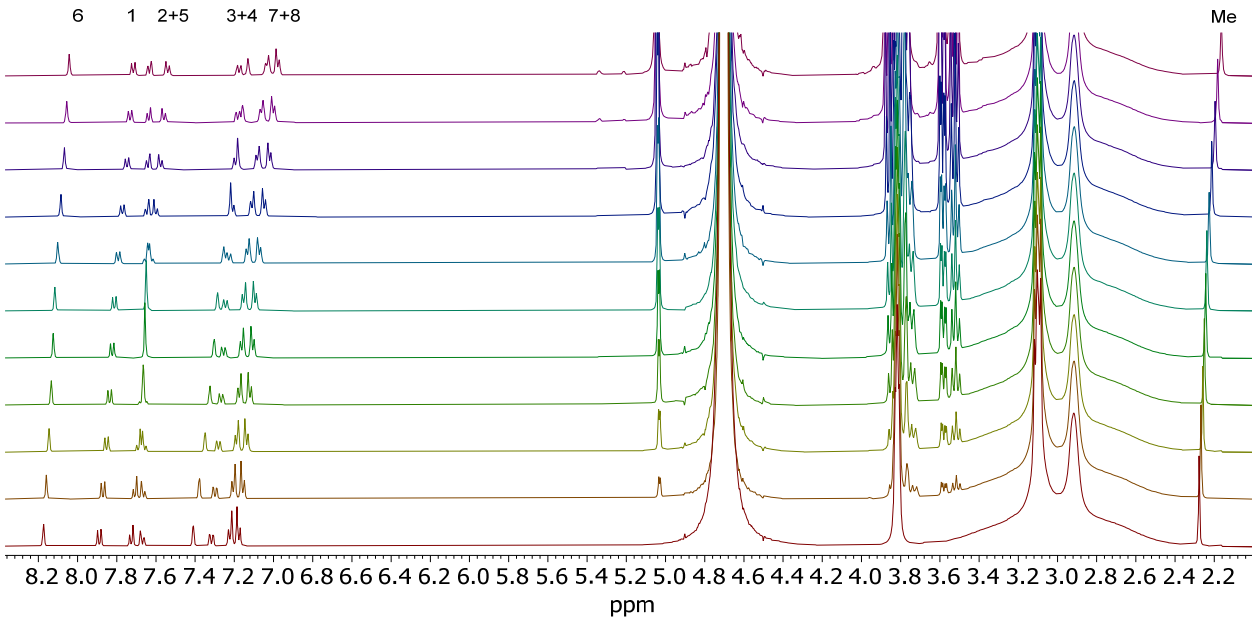

Fig. S16 ^{1}H NMR titration (500 MHz, D_2O/HEPES 5 mM, 25 °C) of TNS (1 mM) with subsequent additions of *γ*-CyD ([*γ*-CyD]=0.1÷2.83 mM).

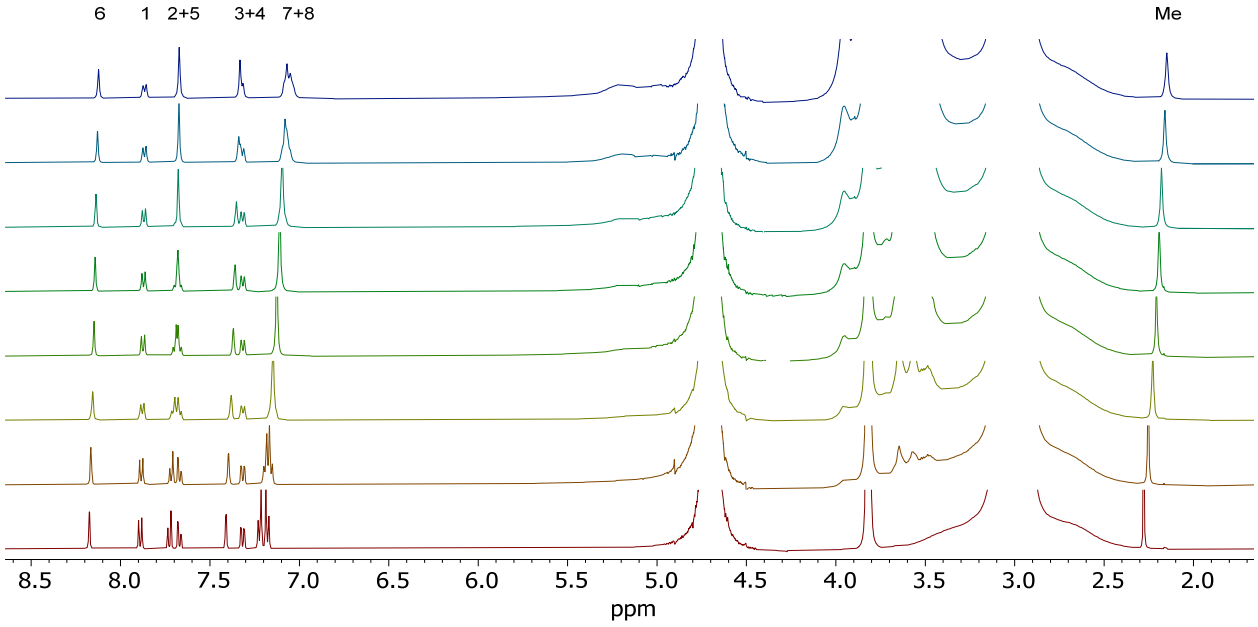

Fig. S17 ^{1}H NMR titration (500 MHz, D_2O/HEPES 5 mM, 25 °C) of TNS (1 mM) with subsequent additions of ***γ*-CyDngs** ([***γ*-CyDngs**]= 0.1 ÷ 2.83 mM).

Notes and references

1 J. K. Oh, D. I. Lee and J. M. Park, *Progress in Polymer Science (Oxford)*, 2009, **34**, 1261–1282.

2 M. Antonietti and K. Landfester, *Progress in Polymer Science*, 2002, **27**, 689–757.

3 M. D. Moya-Ortega, C. Alvarez-Lorenzo, H. H. Sigurdsson, A. Concheiro and T. Loftsson, *Carbohydrate Polymers*, 2012, **87**, 2344–2351.

4 S. Sohn and D. Kim, *Chemosphere*, 2005, **58**, 115–123.

5 J. Catalán, C. Díaz and F. García-Blanco, *J. Org. Chem.*, 2001, **66**, 5846–5852.